Journal Pre-proof

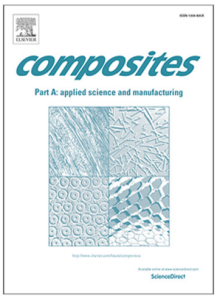

Modeling the effect of temperature and pressure on the peak and steady-state ply-ply friction response for UD C/PAEK tapes

E.R. Pierik, W.J.B. Grouve, S. Wijskamp, R. Akkerman

PII: S1359-835X(23)00247-6
DOI: https://doi.org/10.1016/j.compositesa.2023.107671
Reference: JCOMA 107671

To appear in: *Composites Part A*

Received date : 12 January 2023
Revised date : 10 May 2023
Accepted date : 27 June 2023

Please cite this article as: E.R. Pierik, W.J.B. Grouve, S. Wijskamp et al., Modeling the effect of temperature and pressure on the peak and steady-state ply-ply friction response for UD C/PAEK tapes. *Composites Part A* (2023), doi: https://doi.org/10.1016/j.compositesa.2023.107671.

Modeling the effect of temperature and pressure on the peak and steady-state ply-ply friction response for UD C/PAEK tapes

E.R. Pierik[a,b], W.J.B. Grouve[a,*], S. Wijskamp[b], R. Akkerman[a,b]

[a] *Faculty of Engineering Technology, Chair of Production Technology, University of Twente, Drienerlolaan 5, Enschede, 7522 NB, The Netherlands,*
[b] *ThermoPlastic composites Research Center (TPRC), Palatijn 15, Enschede, 7521 PN, The Netherlands,*

Abstract

A proper description of ply-ply friction is essential for the simulation of thermoplastic composite forming processes. The friction response from characterization experiments typically shows a peak followed by a steady-state shear stress. The rate-dependency of the peak and steady-state shear stress can be predicted by considering shear flow and wall slip effects. In this study, we investigated the temperature- and pressure-dependency of the peak and steady-state friction. The friction decreased slightly with increasing temperature, which was predicted by the shear flow model when including the temperature-dependency of the matrix viscosity. Further, the normal pressure was found to govern the onset of wall slip. A high pressure suppresses wall slip, increasing the steady-state friction. This effect was successfully modeled by including a pressure-sensitive critical shear stress for the onset of wall slip.

Keywords: A. Polymer-matrix composites (PMCs); A. Thermoplastic resin; E. Forming; Friction

*Corresponding author
Email address: w.j.b.grouve@utwente.nl (W.J.B. Grouve)

1. Introduction

First-time-right defect-free manufacturing of continuous fiber-reinforced thermoplastics requires accurate process simulations, in particular on defect generation. In turn, accurate predictions require an accurate description of the formability of a material in constitutive relations. The formability of a material is commonly described by different deformation mechanisms that occur during forming [1, 2], which can be separately characterized and modeled. Three of the most important deformation mechanisms are ply bending, intra-ply shear, and inter-ply slippage. Ply bending is required for forming single curvatures, while doubly-curved parts also require intra-ply shear [3–6]. In general, ply-ply slippage is in both cases essential to avoid defects from occurring, as shown by forming experiments of for example Brands et al. [7] and Sachs et al. [8]. Hence, this study focuses on ply-ply friction of thermoplastic matrix composites (TPC), while recent work on bending and intra-ply shear can be found in e.g. [9–11].

Although studies on ply-ply friction of TPC stretches over more than 30 years [12–19], building a proper understanding of the underlying mechanisms is still part of ongoing research. Experimental work often involves pulling a central ply from a stack of plies in the melt state, resulting in a typical friction response as schematically illustrated in Fig. 1. At sufficiently high sliding rates, a peak shear stress τ_p emerges, followed by a steady-state or long-time shear stress τ_∞.

Recently, we evaluated several hypotheses for the underlying mechanism of the transient friction response of UD tapes [20]. One of the discussed hypothesis, a slip relaxation effect gradually giving rise to wall slip, was deemed as the most probable explanation for the peak behavior as illustrated in Fig. 1. In a follow-up study [21], we successfully applied these insights to predict the measured friction characteristics, i.e. the peak τ_p and long-time shear stress τ_∞, of UD C/PEEK and C/LM-PAEK as function of the applied sliding rate, substantiating the concept of wall slip as the underlying mechanism for the transient ply-ply friction response.

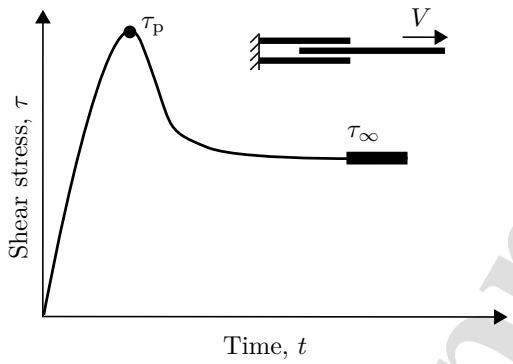

Figure 1: Schematic friction response showing start-up behavior with time [21].

In the current study, we expand the experimental window with respect to our previous work to explore the effect of temperature and normal pressure on the transient friction response. Besides obtaining insights into the effect of these variables on the friction response, the main interest is to validate the shear flow model that we proposed earlier [21]. Specifically, we characterized the ply-ply friction response for UD C/PEEK and C/LM-PAEK at three different temperatures and four normal pressures for a broad range of sliding rates. We found that the shear stress response decreases with increasing temperature. The proposed shear flow model correlates well with the measured data when taking the temperature-dependency of the matrix viscosity into account. An increase in the normal pressure results in higher long-time shear stresses, indicating a suppressing effect of the normal pressure on wall slip, which can be accurately captured through increasing the critical shear stress for the onset of wall slip. A detailed report of the experimental work together with the modeling efforts and discussion will follow, but a brief description of the mentioned shear flow model will be presented first. The reader is kindly referred to [21] for more detail on the modeling aspects.

2. Shear flow through a ply-ply interface

The ply-ply friction response is often said to be viscous in nature due to the assumed interlayer of matrix material between the fibers of adjacent plies [4, 14, 22]. The starting point of our modeling work is, therefore, the assumption of a 1D shear flow of the matrix material through the ply-ply interface, without any flow interference in the width direction [21].

A schematic illustration of a ply-ply cross-section of two adjacent unidirectional plies, both oriented with their fibers in the sliding direction and separated by the x-axis, is shown in the upper-left corner of Fig. 2. The fibers are assumed to be surrounded by the molten matrix material. By introducing a relative movement between both plies through a sliding rate V, a shear rate $\dot{\gamma}$ will be generated in the matrix material depending on the matrix interlayer thickness through $V/h(x)$, as illustrated in the upper-right corner. The local matrix interlayer thickness is not constant due to the fibers at the plies' surfaces, leading to a matrix interlayer thickness distribution $h(x)$ over the width direction (upper graph in Fig. 2). Consequently, a distribution of shear rates will be present in the ply-ply interface upon shearing, as shown in the middle graph. In turn, the shear rate distribution combined with the viscosity of the matrix material $\eta(\dot{\gamma})$ results in a viscous shear stress distribution,

$$\tau_{\mathrm{visc}}(\dot{\gamma}) = \eta\left(\dot{\gamma}\right)\dot{\gamma} \quad \text{with} \quad \dot{\gamma}(x) = \frac{V}{h(x)}, \tag{1}$$

schematically shown in the lower graph of Fig. 2.

As mentioned, we proposed a slip relaxation effect, resulting in a gradual increase of wall slip between the matrix and the fiber surface with the ongoing deformation, as the most probable explanation for the typical (start-up) friction response [20]. Hence, we implemented a second critical shear stress $\tau_{\mathrm{c},2}$ in our shear flow model to locally represent the effect of fully-developed strong wall slip, limiting the local viscous shear stress, in line with findings on pure polymer melts [23–32]. Including $\tau_{\mathrm{c},2}$ as a slip threshold on the viscous shear stress distribution yields:

$$\tau_{\mathrm{visc,slip}}(\dot{\gamma}) = \min\left[\eta\left(\dot{\gamma}\right)\dot{\gamma}, \tau_{\mathrm{c},2}\right], \tag{2}$$

as schematically illustrated by the grey dashed line in the bottom graph of Fig. 2. The value for $\tau_{c,2}$, a material parameter, can be experimentally determined.

The average shear stress in the ply-ply interface can then be obtained through integration of the shear stress distribution over the width w:

$$\tau_{\text{avg}} = \frac{1}{w} \int_0^w \tau(\dot{\gamma}) \, \mathrm{d}x, \tag{3}$$

yielding τ_{avg} for the no-slip shear stress distribution $\tau_{\text{visc}}(\dot{\gamma})$ as given in Equation (1) and $\tau_{\text{avg,slip}}$ when integrating the shear stress distribution with slip $\tau_{\text{visc,slip}}(\dot{\gamma})$ according to Equation (2).

The average shear stresses τ_{avg} and $\tau_{\text{avg,slip}}$ were successfully used to predict the measured peak and long-time shear stress of UD C/PEEK and C/LM-PAEK in our earlier work [21], in which model and measurement were compared in flow curves of shear stress versus the applied rate. We obtained the matrix interlayer thickness distribution in the ply-ply interface by analyzing cross-sectional micrographs of tested specimens. Additionally, the ply-ply interface was mimicked by generated random fiber distributions based on the work of Melro et al. [33], which yielded a good correlation between model and measurement as well. The fiber distribution at the ply-ply interface is especially of influence on the prediction of τ_{∞}, as it dictates, depending on the applied rate, the partition between slip and viscous flow in the ply-ply interface. In this study, the same matrix interlayer thickness distributions were used as in our earlier work [21], as obtained from analyzing generated random fiber distributions.

3. Materials and methods

A description of the materials and equipment used to measure the ply-ply friction response will be given in this section. The procedure for performing the tests is included as well as the experimental conditions. Lastly, we will discuss the inputs for the shear flow model.

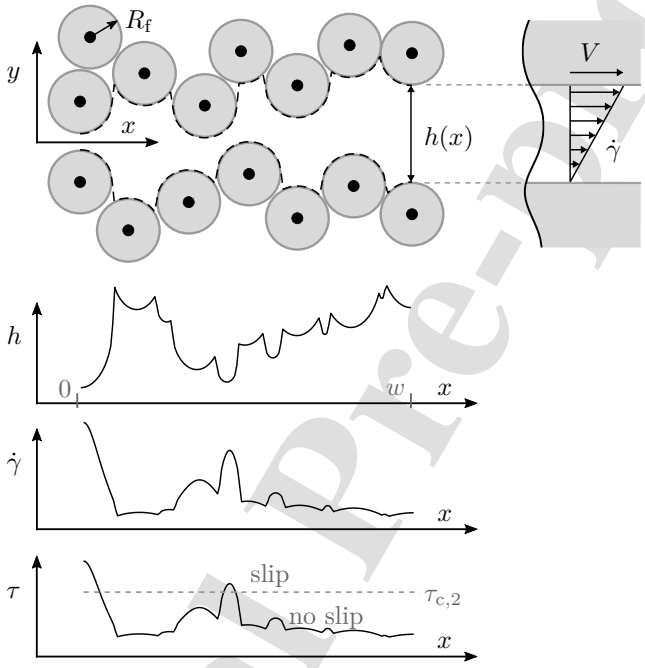

Figure 2: Schematic illustration of a ply-ply cross-section, visualizing the interface between two plies. The fibers of each ply are separated by the x-axis, where the fiber edges above and below this line provide the matrix interlayer thickness distribution $h(x)$, as shown in the upper graph. A shear rate $\dot{\gamma}$ will be generated when the top ply moves with the applied sliding rate V with respect to the lower one (visualized in the upper-right corner), resulting in a distribution of shear rates (middle graph). A shear stress distribution can be computed by considering the matrix viscosity, as shown in the lower graph. The dashed line reflects the effect (strong) wall slip by opposing a critical shear stress $\tau_{c,2}$, which bounds the local viscous shear stress [21].

3.1. Materials

The materials under investigation are manufactured by Toray Advanced Composites [34] and are known as Cetex TC1200 (C/PEEK) and TC1225 (C/LM-PAEK). Both material systems are reinforced with aligned (UD) continuous carbon fibers with a fiber volume fraction of approximately 59%. The melting temperature equals 343 °C for C/PEEK and 305 °C for C/LM-PAEK. The processing temperature range is 370-400 °C and 340-385 °C for C/PEEK and C/LM-PAEK, respectively.

3.2. Rheometry

The neat matrix thermoplastic polymers, Victrex PEEK 150P and Victrex LM-PAEK AE250P, were available in powder form. A plate-plate setup in an Anton Paar MCR501 rheometer was used to measure the shear viscosity. First, an amplitude sweep was applied to identify the linear viscoelastic range, after which a frequency sweep was applied to obtain the complex viscosity as function of the applied frequency. Lastly, the validity of the Cox-Merz rule was checked by means of a strain rate sweep. Viscosity curves were measured at 370, 380, and 390 °C for PEEK and 345, 365, and 385 °C for LM-PAEK, and fitted using the Cross model [35],

$$\eta(\dot{\gamma}) = \frac{\eta_0(T)}{1 + (\frac{\eta_0 \dot{\gamma}}{\tau^*})^{(1-n)}}, \tag{4}$$

with $\eta_0(T)$ the zero shear viscosity, τ^* the critical shear stress, and n the power law index. The temperature dependency of the zero shear viscosity $\eta_0(T)$ was modeled by means of the Arrhenius equation [35],

$$\eta_0(T) = \eta_{0,\text{ref}} \exp\left[\frac{E}{R}\left(\frac{1}{T} - \frac{1}{T_{\text{ref}}}\right)\right], \tag{5}$$

with $\eta_{0,\text{ref}}$ the zero shear viscosity at the reference temperature T_{ref}, R the universal gas constant, and E the activation energy, which was treated as a fitting parameter.

3.3. Ply-ply friction tests

3.3.1. Friction setup and procedure

The ply-ply friction experiments were conducted at the University of Twente on a benchmarked, purpose-built setup [19]. A schematic illustration of the friction tester is shown in Fig. 3, which was placed in a universal testing machine. The pre-preg UD tapes were first cut in strips measuring 250×50 mm^2 and 120×50 mm^2 for the central and outer plies, respectively, with the fibers aligned with the length direction. A single central ply was clamped at the upper clamp of the universal testing machine, while the outer plies were clamped at the bottom. The three plies were stacked between pressure platens with contact area A (50×50 mm^2), resulting in two ply-ply interfaces as visualized in Fig. 3. Alignment of the specimen was checked using a laser leveler. A normal force F_n was applied on the pressure platens and the temperature of these platens was actively controlled. Metal foils were used to protect the pressure platens from the molten polymer, which were fixed together with the outer plies at the lower clamp of the friction tester. The central ply was mounted with an additional 15 mm overlap to ensure sufficient material at the inlet for a pull-trough test (see Fig. 3).

The resistance against slippage was characterized by imposing a certain constant sliding rate V and measuring the pulling force F_pull and displacement d with time t. The average shear stress per interface can then be obtained via:

$$\tau = \frac{F_\mathrm{pull}}{2A}, \tag{6}$$

where A is the contact area. Note that the coefficient of friction can be calculated by dividing the shear stress by the applied normal pressure.

When the sliding movement was stopped after a displacement of around 10 mm, force logging continued to record the subsequent shear stress relaxation as well. Earlier research has shown that a residual stress τ_y is present after full relaxation [14, 21], attributed to fiber-fiber interaction [22, 36, 37]. We used this residual stress to compute the viscoelastic matrix contribution τ_mat from

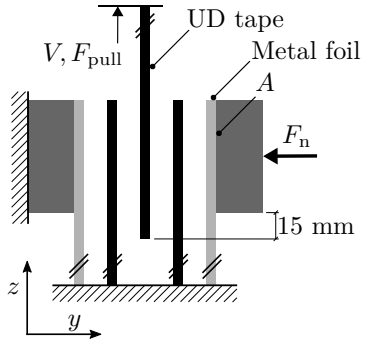

Figure 3: Schematic illustration of the friction tester used to characterize the ply-ply friction response of pre-preg UD tape by forcing (F_{pull}) a central ply, clamped at the upper clamp of a universal testing machine, to slide at a constant rate V against stationary outer plies, clamped at the bottom. A normal pressure was applied through a force F_{n} on the pressure platens (dark grey) with contact area A, which were heated [21].

the total measured shear stress:

$$\tau = \tau_{\text{y}} + \tau_{\text{mat}}. \tag{7}$$

The ply-ply friction observations on τ_{y} reported by Murtagh et al. [14] suggest that we can safely assume that τ_{y} remains constant throughout the whole test. The observed values are typically in the range of 1 kPa for the materials considered in this research [13, 14, 21]. The viscoelastic matrix contribution τ_{mat} will be the focus of the remainder of this work, as our earlier research [21] showed the correlation between this contribution and the viscous matrix interlayer in the ply-ply interface. To conclude the testing procedure, the bottom clamp was loosened after around 1 minute of relaxation, and the final force reading was used to zero the force. The reader is kindly referred to references 2, 38, 39 for more detail on the friction tester.

3.3.2. Experimental conditions

Friction tests were performed at a certain constant temperature T and normal pressure p for a range of sliding rates V ($1 - 200$ mm/min), such that a flow curve of shear stress versus applied rate could be constructed. Different

Table 1: Overview of tested temperature and pressure conditions for C/PEEK and C/LM-PAEK.

	Temperature tests		Pressure tests	
	T [°C]	p [kPa]	T [°C]	p [kPa]
C/PEEK	370, 385, 400	15	385	5, 15, 45, 135
C/LM-PAEK	345, 365, 385	15	365	5, 15, 45, 135

temperature and normal pressure conditions were tested, which are provided in Table 1. The test temperatures align with the processing conditions as advised by the manufacturer [34] and the normal pressure conditions were selected based on earlier studies [2, 5, 14, 17, 19, 40–42]. The actual normal pressures during forming are expected to change from zero to possibly very high values, though the ply-ply slippage is anticipated to take place in the early stage of the forming process where the pressures are still relatively low.

For C/PEEK, measurements were conducted at temperatures of 370, 385, and 400 °C at a reference normal pressure of 15 kPa. Subsequently, the normal pressure was varied over 5, 45, and 135 kPa at a reference temperature of 385 °C. A lower temperature range of 345, 365, and 385 °C was chosen for C/LM-PAEK with equal reference normal pressure of 15 kPa. The same range of normal pressures was measured as considered for C/PEEK at a reference temperature of 365 °C. Thus, six conditions were tested per material, with a range of sliding rates for each condition, summing up to a total of 136 experiments per material. The measurements at the reference conditions were part of our previous work [21], while the current work enlarges the scope to the effect of the temperature and normal pressure on the friction response for both materials.

3.4. Shear flow model

The shear flow model as outlined in Section 2 was used to predict the measured peak $\tau_{\mathrm{mat,p}}$ and long-time shear stress $\tau_{\mathrm{mat},\infty}$ with a no-slip and slip boundary condition, respectively. The no-slip shear-stress predictions were ob-

tained through Equations (1) and (3), requiring two model inputs: the matrix interlayer thickness distribution $h(x)$ and the matrix viscosity. The shear-stress prediction with slip, using Equations (2) and (3), requires in addition a critical shear stress $\tau_{c,2}$. The matrix interlayer thickness distributions used for both predictions were based on ten generated fiber distributions using the algorithm of Melro et al. [33] to mimic the ply-ply interface. The random fiber distributions were generated with a fiber diameter d_f of 7 µm and a fiber volume fraction V_f of 59% in a rectangle of $10d_f$ high and $50d_f$ wide. The ten fiber distributions were subsequently evaluated following the analysis as presented in our earlier work [21] to obtain ten different matrix interlayer thickness distributions $h(x)$. As each of the computed matrix interlayer thickness distributions results in a τ_{avg} and $\tau_{avg,slip}$, the means were calculated to obtain $\bar{\tau}_{avg}$ and $\bar{\tau}_{avg,slip}$. The combined Cross-Arrhenius model was used to represent the shear thinning viscosity at the corresponding temperature, such that the temperature effect on the matrix viscosity was taken into account. The critical shear stress for onset of strong wall slip $\tau_{c,2}$ was set equal to the experimentally measured $\tau_{mat,\infty}$-plateau value.

4. Results

This section starts with the rheometry results, after which the ply-ply friction findings will be presented together with the modeling outcomes.

4.1. Rheometry

The effects of shear rate and temperature on the viscosities of PEEK 150P and LM-PAEK AE250P are shown in Fig. 4a and 4b, respectively. For each material, the viscosity curves were fit with the Cross model (Equation (4)), of which the zero-shear viscosities η_0 were used to model the temperature dependency with the Arrhenius Equation (5). The lowest temperature was used as the reference temperature with corresponding reference viscosity, leaving only the activation energy E as a fitting parameter for the temperature dependency.

The viscosity representation of the combined Cross-Arrhenius model is plotted in Fig. 4 by the solid lines, for which the Cross model parameters τ^* and n as fit at the intermediate temperature (i.e. 380 and 365 °C for PEEK and LM-PAEK, respectively) were used. The fitting parameters per material are mentioned in the caption of Fig. 4. A good correlation was found between the extrapolated model viscosity and capillary rheometry data of LM-PAEK, kindly provided by the manufacturer Victrex plc. [43], at high rates. Note that the poor correlation at low rates is probably due to the capillary data becoming unreliable at these lower rates, as suggested by the manufacturer.

4.2. Ply-ply friction tests

The typical friction response exhibits a peak τ_p and long-time shear stress τ_∞, as indicated in Fig. 1. These two stresses were extracted from the viscoelastic matrix contribution of the measured friction data, according to Equation (7), and plotted as function of the applied rate to obtain flow curves. The flow curves of C/PEEK for different temperatures at the reference normal pressure of 15 kPa are shown in Fig. 5, in which the triangles represent the peak $\tau_{\mathrm{mat,p}}$ and the circles the long-time shear stress $\tau_{\mathrm{mat},\infty}$.

The applied rate V has a strong effect on the measured shear stress, with both $\tau_{\mathrm{mat,p}}$ and $\tau_{\mathrm{mat},\infty}$ gradually increasing with rate. While $\tau_{\mathrm{mat,p}}$ keeps increasing, $\tau_{\mathrm{mat},\infty}$ is bounded by a limiting value at higher rates, resulting in a rate-independent $\tau_{\mathrm{mat},\infty}$, and consequently a $\tau_{\mathrm{mat},\infty}$-plateau emerges. Hence, large differences between $\tau_{\mathrm{mat,p}}$ and $\tau_{\mathrm{mat},\infty}$ can be observed at high rates, while no difference is seen at low rates. The friction response at low rates increased monotonically towards the stationary value without showing a peak. Hence, $\tau_{\mathrm{mat,p}}$ and $\tau_{\mathrm{mat},\infty}$ were both evaluated at the first sign of a steady-state regime at low rates.

The effect of temperature is small when comparing the flow curves shown in Fig. 5. Overall, the peak and long-time shear stress flow curves all look similar and the $\tau_{\mathrm{mat},\infty}$-plateau is barely affected, while a slight increase in peak shear stress with decreasing temperature T can be observed. This slight increase is

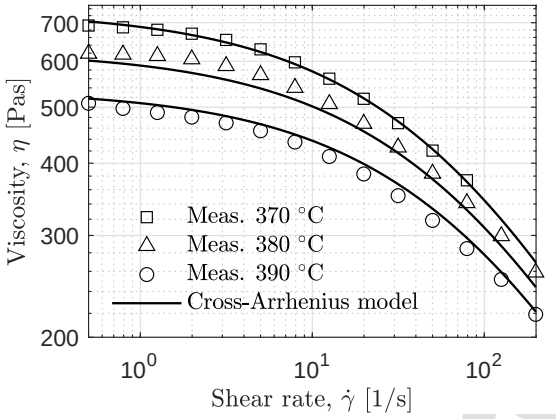

(a)

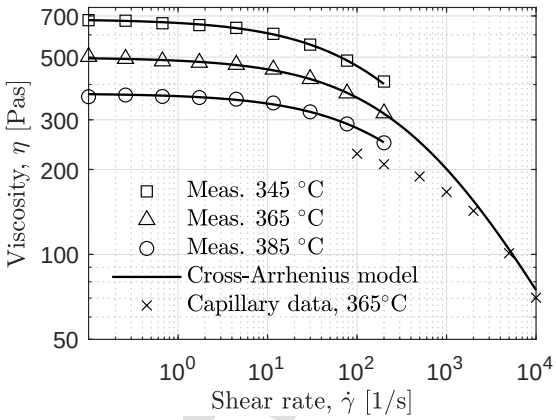

(b)

Figure 4: Measured viscosity versus shear rate for different temperatures of (a) PEEK 150P with Cross-Arrhenius model output at corresponding temperatures ($\tau^* = 6.05\text{e}4$ Pa, $n = 0.38$, $\eta_{0,\text{ref}} = 733.67$ Pas, and $E = 5.57\text{e}4$ J/mol using a reference temperature of 370 °C) and (b) LM-PAEK AE250P with Cross-Arrhenius model ($\tau^* = 2.53\text{e}5$ Pa, $n = 0.42$, $\eta_{0,\text{ref}} = 681.90$ Pas, and $E = 5.13\text{e}4$ J/mol using a reference temperature of 345 °C).

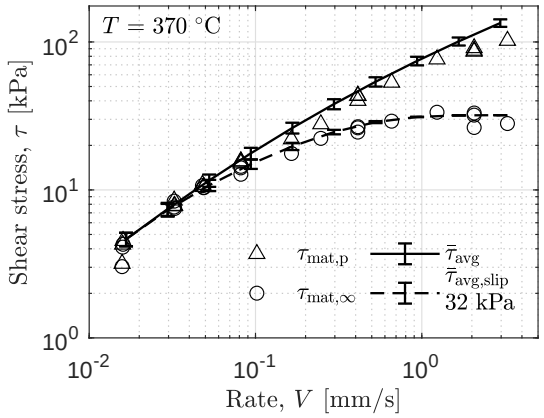

(a)

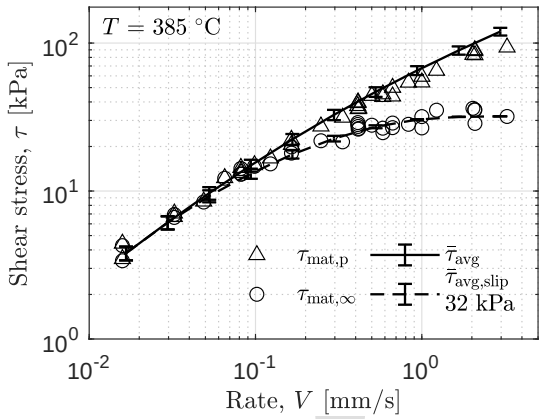

(b)

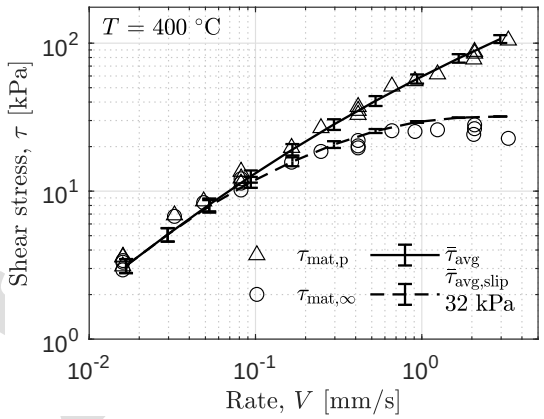

(c)

Figure 5: Measured peak (triangles) and long-time (circles) shear stress of the matrix contribution for C/PEEK at a normal pressure of 15 kPa and a temperature of (a) 370, (b) 385 (reproduced from [21]), and (c) 400 °C. The solid lines represent the mean peak shear-stress predictions for ten matrix interlayer thickness distributions, while the dashed lines represent the predictions including the effects of fully-developed strong wall slip. The error bars denote the standard deviation.

due to the viscosity change of the matrix material in the ply-ply interface, which we consider in the shear flow model.

Shear-stress predictions of the shear flow model, as described in Section 2, are included as well in the flow curves of Fig. 5. The solid lines represent the no-slip prediction, whereas the dashed lines represent the condition with strong slip. The error bars indicate the standard deviation over the ten matrix interlayer thickness distributions used. A good correlation was found between the no-slip prediction $\bar{\tau}_{avg}$ and the measured peak shear stress $\tau_{\mathrm{mat,p}}$. The predictions slightly overestimate the measured peak shear stress at high rates, especially for the flow curve at the lowest temperature (see Fig. 5a). Further, the prediction including fully-developed strong wall slip $\bar{\tau}_{\mathrm{avg,slip}}$ correlates well with the measured long-time shear stress $\tau_{\mathrm{mat},\infty}$. The critical shear stress $\tau_{\mathrm{c},2}$ was set equal to 32 kPa for all three temperature conditions according to the average measured $\tau_{\mathrm{mat},\infty}$-plateau. Note that $\tau_{\mathrm{c},2}$ locally acts as a threshold between no-slip and slip in the ply-ply interface, while the distribution of $h(x)$ dictates the global transition from no-slip to full-slip with increasing rate. This slip transition with rate results in an accurate description of the measured rate-dependency of $\tau_{\mathrm{mat},\infty}$.

Fig. 6 shows the flow curves of C/LM-PAEK for 345, 365, and 385 °C. The triangles denote again the peak shear stress $\tau_{\mathrm{mat,p}}$, while the circles denote the long-time shear stress $\tau_{\mathrm{mat},\infty}$. Similar observations as made with C/PEEK apply to the C/LM-PAEK flow curves, including the appearance of a $\tau_{\mathrm{mat},\infty}$-plateau at higher rates. The predictions of the shear flow model are included by the solid (no-slip) and dashed (slip) lines, based on the same ten matrix interlayer thickness distributions. A good correlation with the measured data is again obtained when using the viscosity of LM-PAEK AE250P at the corresponding temperatures. Especially the prediction at low rates corresponds well with the measured data, while the overprediction of the peak shear stress at high rates is slightly larger compared with C/PEEK. The transition from no-slip to full-slip with increasing rate (dashed line) agrees well with the measured $\tau_{\mathrm{mat},\infty}$. For this material, the critical shear stress was set equal to 55 kPa for all three

temperature conditions based on the measured $\tau_{\mathrm{mat},\infty}$-plateau.

The good correlation between model and measurement for each of the three temperature conditions and both material systems demonstrates the applicability of the shear flow model to describe the characteristics of the ply-ply friction response. The slight increase in measured shear stress with decreasing temperature, seen with both material systems, is accurately calculated when using the temperature dependency of the matrix material.

Next, the flow curves of C/PEEK and C/LM-PAEK for different normal pressures of 5, 45, and 135 kPa are shown in Fig. 7 and 8, respectively. Note that the flow curves at the reference normal pressure of 15 kPa are already shown in Fig. 5b and 6b for C/PEEK and C/LM-PAEK, respectively.

The long-time shear stress $\tau_{\mathrm{mat},\infty}$ was significantly affected by the normal pressure. The $\tau_{\mathrm{mat},\infty}$-plateau shifts towards higher stresses and rates with increasing normal pressure, as can be seen when comparing for example the flow curves at 5 and 135 kPa of C/PEEK (Fig. 7a and 7c, respectively). Further, when looking at the same flow curves, an overall increase in shear stress with increasing normal pressure can be observed in especially the lower rate range. The shear stress increase can also be observed in the C/LM-PAEK data when comparing Fig. 8a and 8c measured at 5 and 135 kPa, respectively, though the effect is a bit smaller compared with the C/PEEK data. A more striking observation in the C/LM-PAEK data is the drop in long-time shear stress after the $\tau_{\mathrm{mat},\infty}$-plateau at the highest rate and lowest normal pressure of 5 kPa (Fig. 8a), which is to a lesser extent also present in the C/PEEK data (Fig. 7a).

The shear flow model was applied once again to describe the measured characteristics of the friction response, again using the same ten matrix interlayer thickness distributions and the combined Cross-Arrhenius model for the matrix viscosity at 385 and 365 °C for C/PEEK and C/LM-PAEK, respectively, irrespective of the applied normal pressure. Hence, the predicted no-slip flow curves, corresponding to $\tau_{\mathrm{mat,p}}$ and represented by the solid lines, remain the same regardless of the normal pressure conditions. A fair correlation between model and measurement was obtained. However, the response at the highest

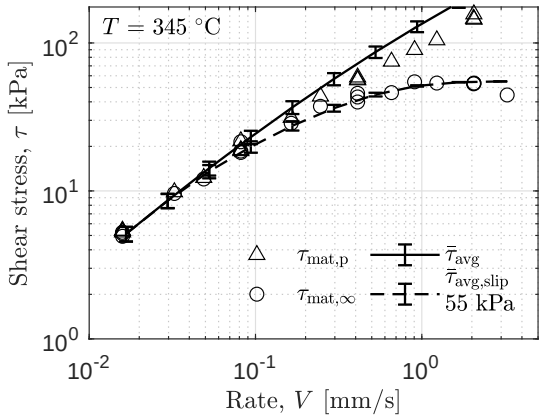

(a)

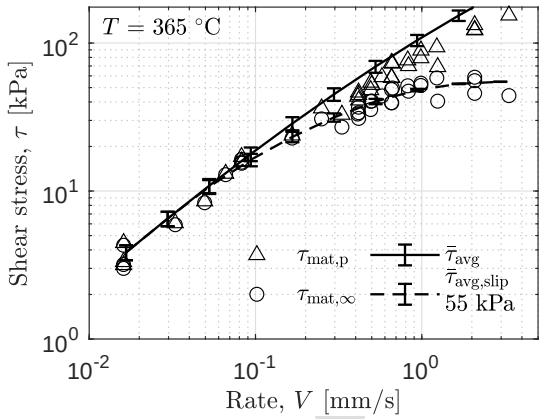

(b)

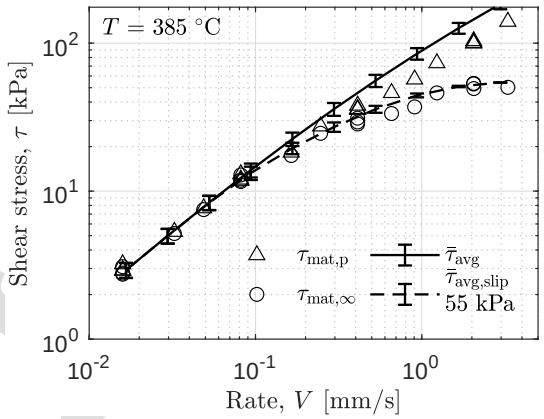

(c)

Figure 6: Measured peak (triangles) and long-time (circles) shear stress of the matrix contribution for C/LM-PAEK at a normal pressure of 15 kPa and a temperature of (a) 345, (b) 365 (reproduced from [21]), and (c) 385 °C. The solid lines represent the mean peak shear-stress predictions for ten matrix interlayer thickness distributions, while the dashed lines represent the predictions including the effects of fully-developed strong wall slip. The error bars denote the standard deviation.

normal pressure is underpredicted, especially for C/PEEK as shown in Fig. 7c.

Contrary to the $\tau_{\mathrm{mat,p}}$ predictions, the flow curve predictions for $\tau_{\mathrm{mat},\infty}$, represented by the dashed lines, do change with the applied normal pressure. Namely, $\tau_{\mathrm{c},2}$ increases with an increasing normal pressure to accurately describe the change in slip behavior as seen by the increase in the $\tau_{\mathrm{mat},\infty}$-plateau. The distribution of thicknesses in the matrix interlayer $h(x)$ is still able to accurately account for the transition from no-slip at low rates towards the (almost) full-slip condition at high rates. Only the prediction for C/PEEK at the highest normal pressure of 135 kPa (Fig. 7c) fails, due to the overall increase in friction as mentioned earlier.

5. Discussion

We will discuss the ply-ply friction experimental and modeling results by separately addressing the effects of the sliding rate, temperature and, in particular, the normal pressure.

5.1. The effect of rate

The flow curves of C/PEEK and C/LM-PAEK as visualized in Fig. 5 to 8 show an increase in friction with a stronger peak behavior, as the difference between the peak and long-time values becomes larger, with increasing rate. These observations align with earlier findings on friction of TPC in melt (e.g. [2, 5, 14–17, 40, 41, 44, 45]). Furthermore, the long-time shear stress $\tau_{\mathrm{mat},\infty}$ flow curves show a $\tau_{\mathrm{mat},\infty}$-plateau, indicating that the stationary values in the friction experiments became rate-independent at these high rates. Sachs [2] reported this rate-independency of the long-time shear stress as well in a study on tool-ply friction of UD C/PEEK.

The observed peak response and the rate-independency of the stationary values strongly resemble experimental findings on shear flow of pure polymer melts suffering from wall slip [25, 28, 29, 46–48]. For example, Boukany and Wang [48] used a sliding plate with particle tracking velocimetry to show that

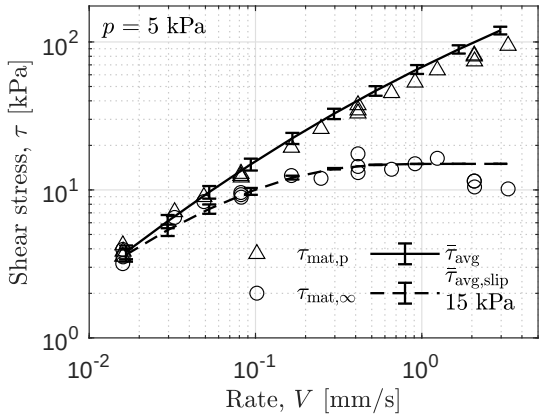

(a)

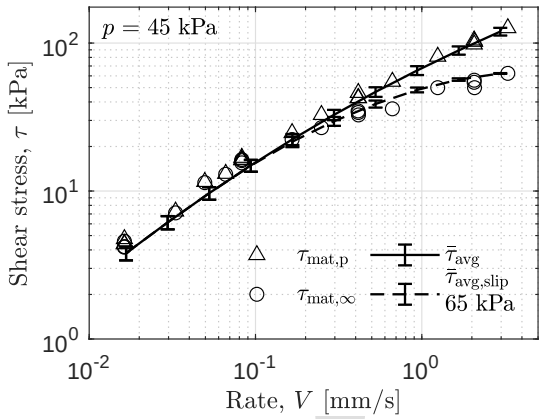

(b)

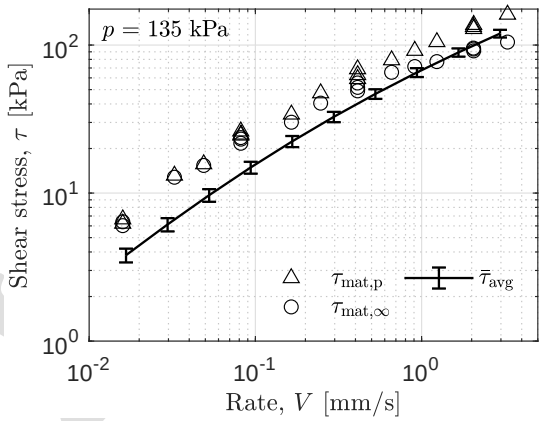

(c)

Figure 7: Measured peak (triangles) and long-time (circles) shear stress of the matrix contribution for C/PEEK at a temperature of 385 °C and a normal pressure of (a) 5, (b) 45, and (c) 135 kPa. The solid lines represent the mean peak shear-stress predictions for ten matrix interlayer thickness distributions, while the dashed lines represent the predictions including the effects of fully-developed strong wall slip. The error bars denote the standard deviation.

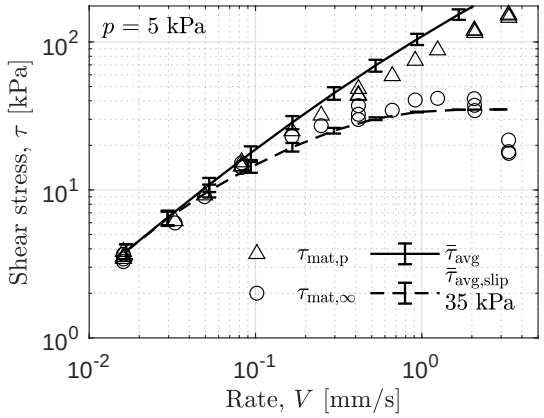

(a)

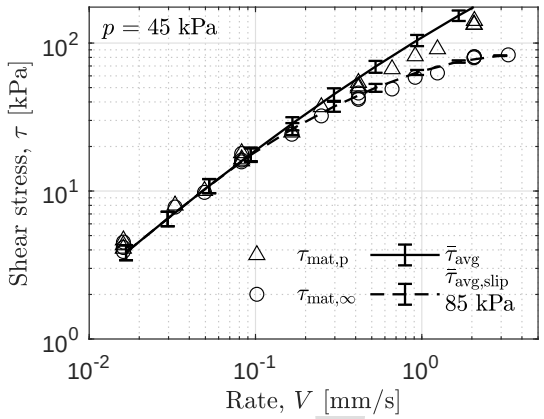

(b)

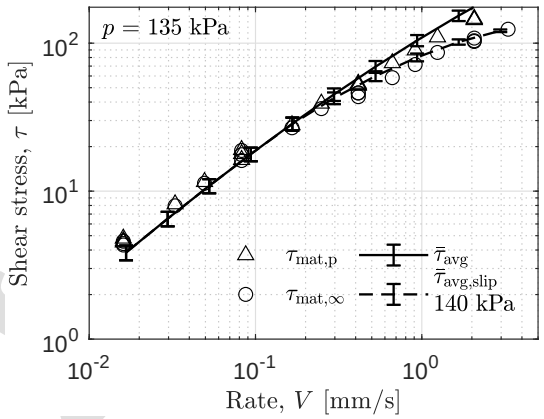

(c)

Figure 8: Measured peak (triangles) and long-time (circles) shear stress of the matrix contribution for C/LM-PAEK at a temperature of 365 °C and a normal pressure of (a) 5, (b) 45, and (c) 135 kPa. The solid lines represent the mean peak shear-stress predictions for ten matrix interlayer thickness distributions, while the dashed lines represent the predictions including the effects of fully-developed strong wall slip. The error bars denote the standard deviation.

the measured peak shear stress of a well entangled polymer melt (polyisoprene) was accompanied by a change in the velocity profile form linear towards one with slip near the wall. They reported that besides a high rate, also sufficient deformation is required to establish this new boundary condition. Thus, the first response is primarily dominated by viscoelastic effects of the polymer melt, which is substantiated in this study by the good correlation between predictions of the shear flow model and the measured peak shear stress when assuming a no-slip condition at the fiber-matrix interface. The prediction especially holds for low rates, while the model starts to overpredict the measured peak shear stress at the highest rates. This overprediction at high rates was also seen in our earlier work [21], in which we suggested that a small degree of slip could already be developed when measuring the peak friction, conflicting with the no-slip assumption.

Mhetar and Archer [29] also observed a peak followed by a steady-state response for polybutadiene melts. They reported that the steady-state response was limited to a certain critical shear stress. Hence, the steady-state shear stress remained constant with increasing rates, consequently resulting in increasing slip velocities. Similar findings were reported by Léger et al. [49] on shear flow of highly entangled poly(styrene-butadiene) melts, who also observed a limiting stationary shear stress, in line with our finding of a $\tau_{\mathrm{mat},\infty}$-plateau. As described in Section 2, the origin of this $\tau_{\mathrm{mat},\infty}$-plateau can be found in disentanglement of polymer chains in the bulk from the ones that are adsorbed at the wall [23–25]. This disentanglement process or strong slip occurs at a certain second critical shear stress $\tau_{\mathrm{c},2}$. The correlation between model and measurement when solely accounting for $\tau_{\mathrm{c},2}$ as a measure for wall slip substantiates the idea of a slip-relaxation effect in the fiber-matrix interface.

5.2. The effect of temperature

The effect of temperature on the friction response for C/PEEK and C/LM-PAEK is shown in Fig. 5 and 6, respectively, with shear-stress predictions for the peak (solid lines) and long-time shear stress (dashed lines). The inclusion of

the temperature dependency of the zero-shear viscosity led to a good correlation between model and measurement, indicating once again the viscous nature of ply-ply friction as stated in earlier research [4, 5, 14, 22]. The critical shear stress $\tau_{c,2}$ for strong slip differed between the materials yet remained constant between the temperature conditions. Based on research on pure polymers, one might expect stronger slip behavior [31, 50] with a faster transition [25, 48, 51] and thus possibly lower peaks at higher temperatures, but the experimental data in the chosen temperature window is not conclusive enough on this aspect.

5.3. The effect of normal pressure

The effect of the applied normal pressure on the measured long-time shear stress of the matrix contribution $\tau_{mat,\infty}$ is visualized in Fig. 7 and 8 for C/PEEK and C/LM-PAEK, respectively. Both materials show an increase in $\tau_{mat,\infty}$ with increasing normal pressure, which was also observed by Sachs [2], Murtagh et al. [14], and Morris and Sun [15] on friction of UD C/PEEK as well as for other material systems [5, 17, 42].

5.3.1. Shear-stress predictions

An increase in the normal pressure resulted in smaller differences between $\tau_{mat,p}$ and $\tau_{mat,\infty}$ as the $\tau_{mat,\infty}$-plateau shifted towards higher rates and stresses, indicating a suppressing effect of the normal pressure on wall slip (see Fig. 7 and 8). We accounted for this suppressing effect in the shear flow model through increasing $\tau_{c,2}$ according to the measured $\tau_{mat,\infty}$-plateau, resulting in accurate predictions for $\tau_{mat,\infty}$. At the highest normal pressure, no clear $\tau_{mat,\infty}$-plateau emerged within the range of the applied sliding rate (see Fig. 8c), but we expect this plateau to emerge at even higher rates. Therefore, the used $\tau_{c,2}$ was set higher than the measured $\tau_{mat,\infty}$ such that the shear flow model described the measured data accurately. Note that the transition from no-slip to slip with rate, i.e. the shape of the flow curve, is primarily dictated by the distribution of thicknesses in the matrix interlayer $h(x)$. The transition was accurately described for the different normal pressure conditions, while we kept the matrix

interlayer thickness distributions equal.

A plot of $\tau_{c,2}$ as function of the applied normal pressure is shown in Fig. 9 for both materials. No data entry exists for C/PEEK at a normal pressure of 135 kPa, as the shear flow model is not able to capture the overall friction increase measured at this high normal pressure as mentioned earlier. The increase in $\tau_{c,2}$ with increasing normal pressure was also reported by Hatzikiriakos and Dealy [52] in a study on pure polymer melts in a capillary rheometer, though the exact origin remained unclear.

The shear-stress prediction for the peak response correlates well with the measured data, especially at the lower rates. The lower normal pressure resulted in a larger overprediction at high rates (see Fig. 8a) than the one at a higher normal pressure (see Fig. 8c). This increase in overprediction of the peak shear stress with decreasing normal pressure could be due to the stronger slip behavior at a lower normal pressure, as the critical shear stress reduced as well, possibly resulting in already a small degree of slip when the peak friction was measured at these high rates.

5.3.2. Drop after $\tau_{mat,\infty}$-plateau

The flow curves at the lowest normal pressure of 5 kPa, visualized in Fig. 7a and 8a for C/PEEK and C/LM-PAEK, respectively, showed a wide $\tau_{mat,\infty}$-plateau with a drop in $\tau_{mat,\infty}$ at high rates. Such a drop is also seen in the study of Sachs [2] on tool-ply friction of UD C/PEEK as well as in the sliding plate rheometry measurements of Park et al. [27] on a pure polymer melt.

We believe that the presence of a $\tau_{mat,\infty}$-plateau is due to strong slip based on the resemblance with findings on pure polymer melts (e.g. [25, 27–30, 32, 53]) and the successful application of a critical shear stress in our shear flow model. In that way, the $\tau_{mat,\infty}$-drop at high rates implies that the equilibrium shear stress at the interface reduces with increasing rate, suggesting a rate-dependent critical shear stress.

The critical shear stress relates to the disentanglement of polymer chains adsorbed at the surface from the bulk ones [25, 54], following an early study

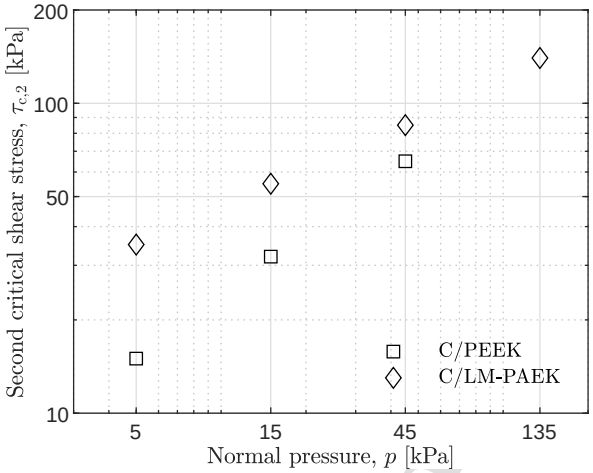

Figure 9: The used second critical shear stress $\tau_{c,2}$ plotted with the applied normal pressure for C/PEEK (squares) and C/LM-PAEK (diamonds). Note that $\tau_{c,2}$ was not determined for C/PEEK at 135 kPa due to the overall friction increase measured at that high normal pressure (see Fig. 7c).

of Brochard and de Gennes [55], in which a model was proposed to describe the shear flow of a polymer melt near a wall with grafted polymer chains. In case of low rates, these grafted chains are well entangled with the bulk chains and provide momentum transfer. At higher rates, the coiled surface chains become stretched and may disentangle. As the coil-stretch transition is related to the applied force, a jump in the measured rate can be observed at a critical shear stress in case of force-controlled experiments. This shear-rate jump was observed in, for example, the experimental work of Boukany et al. [30] and Hatzikiriakos and Dealy [52] using sliding plate and capillary rheometry on an entangled polymer melt. The coil-stretch transition was recently visualized by Kirk et al. [56] in a molecular dynamics simulation.

The forced disentangled of surface chains could also be induced in rate-controlled experiments if sufficient shear rate is applied. Once a surface chain is disentangled, it may relax due to the lower friction experienced [55]. This chain relaxation enables re-entanglement with the bulk chains if the relative velocity

between the surface and bulk chains is sufficiently small, resulting again in a higher interfacial friction and consequently stretching of the surface chains. Hence, there will be a range of rates at which chains dis- and re-entangle in case of rate-controlled experiments, labeled as the marginal state [55]. This marginal state is marked by a constant shear stress and, therefore, a shear stress plateau emerges when constructing the corresponding flow curve. The accompanying slip velocities will gradually increase with increasing rate. Experimental results showed the existence of such a plateau [27–29, 32].

The marginal state ends at a certain rate when re-entanglement of the disentangled surface chain becomes unfavorable due to a high slip velocity, leading to a disentangled layer [55]. This fully disentangled state results in a lower friction, as it is formed by monomer-monomer or Rouse friction rather than entanglements. Capillary experiments on pure polymers have shown this state of low friction [27, 52], but the marginal regime can be better investigated with rate-controlled experiments. For instance, Park et al. [27] found that the discontinuity in the flow curve at the second critical shear stress was followed by a decreasing shear stress with increasing rate and a similar observation was made by Léger et al. [49]. A marginal regime followed by a fully disentangled state at higher rates could explain the observed drop in $\tau_{\mathrm{mat},\infty}$ after the plateau as observed in Fig. 7a and 8a.

5.3.3. Squeeze flow at high normal pressure

The overall shear stress response of C/PEEK increased with increasing normal pressure, as seen when comparing the measured flow curves at the different normal pressure conditions (see Fig. 7). The same observation can be made from the results on C/LM-PAEK, albeit less pronounced (Fig. 8). Furthermore, the ply-ply friction measurements with C/PEEK at a high normal pressure of 135 kPa resulted in a higher shear stress than expected from the shear flow model, as shown in Fig. 7c. We observed that the width of the C/PEEK specimens increased (approximately 1 mm on an initial width of 50 mm) after testing at 135 kPa, which was not or hardly seen with specimens measured at a lower

normal pressure. This width increase indicates that the material was squeezed out from between the pressure platens.

Possibly, the observed macroscopic squeeze flow is accompanied by a change in the local matrix interlayer thickness in the ply-ply interface. The high normal pressure could force a closer fiber packing and reduce the matrix interlayer in the ply-ply interface, consequently lowering the matrix interlayer thickness distribution $h(x)$. In turn, an overall decrease in $h(x)$ may explain the shear-stress underprediction of the shear flow model, as a smaller than expected matrix interlayer thickness will result in higher viscous shear stresses. Analysis of cross-sectional micrographs of a tested specimen did indeed show a smaller matrix interlayer thickness. Consequently, the shear-stress prediction increased (not shown here). The discrepancy between model and measurement, however, did not vanish as the predicted values were roughly between the measured data and the shear-stress prediction based on the default $h(x)$ as shown earlier (see Fig. 7c). Therefore, we used a scale factor of one half instead to reduce $h(x)$. This arbitrary manipulation of the default $h(x)$ may not reflect the actual matrix interlayer thickness distribution present during actual measurements. Other mechanisms that are not included in the proposed shear flow model may become relevant at a high normal pressure, though the resulting shear-stress predictions for the measured peak shear stress $\tau_{\mathrm{mat,p}}$ (triangle symbols) and the long-time shear stress $\tau_{\mathrm{mat},\infty}$ (circles) are quite accurate as shown by the solid and dashed black line in Fig. 10, respectively. The peak shear-stress prediction using the default $h(x)$ is represented by the solid grey line.

6. Conclusion

We investigated the peak and steady-state or long-time shear stress of the transient (start-up) ply-ply friction response of UD C/PAEK tapes using rate-controlled sliding experiments. Both the peak and long-time friction increased with increasing sliding rate, though the long-time shear stress was limited at higher rates resulting in a shear stress plateau in a flow curve of shear stress

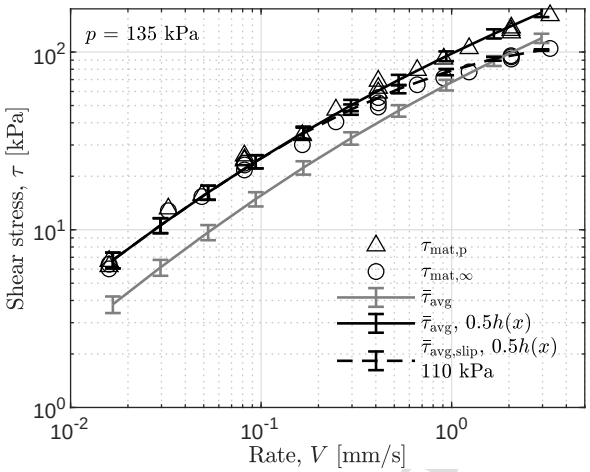

Figure 10: Flow curves of measured peak (triangles) and long-time shear stress (circles) of C/PEEK at 385 °C and 135 kPa with shear-stress predictions based on the ten default matrix interlayer thickness distribution $h(x)$ (grey line) and based on the same ten thickness distributions scaled by 0.5 to mimic a closer packing with no-slip (solid black line) and slip condition (dashed black line). The error bars denote the standard deviation.

versus applied rate. An earlier proposed shear flow model was able to predict the rate-dependency of the measured peak shear stress using the matrix viscosity and a matrix interlayer thickness distribution in the ply-ply interface based on generated fiber distributions. The long-time shear stress was accurately modeled as well when considering local strong wall slip in the ply-ply interface through a critical shear stress, acting as a threshold between no-slip or viscous flow and the slip condition.

Several flow curves were generated to investigate the effect of temperature and normal pressure. As the temperature increased, the shear stresses decreased, but the increase in temperature did not alter the overall slip behavior significantly. Good correlations between model and measurement were obtained by including the temperature-dependency of the matrix viscosity. The normal pressure did affect the slip behavior, as the long-time shear stress plateau shifted towards higher stresses and rates with increasing normal pressure. The shear

flow model was able to accurately describe these flow curves by increasing the critical shear stress for the onset of strong slip, indicating a suppressing effect of the higher normal pressure on the slip behavior.

In conclusion, we showed that the concept of wall slip in the form of strong slip explains the observed ply-ply friction behavior for different conditions of temperature and normal pressure. These findings will help to develop a constitutive model that describes the transient (start-up) ply-ply friction response for the purpose of simulation software.

Acknowledgments

This work was performed as part of the MaterialenNL research program under project number 17880, which is financed by the Dutch Research Council (NWO). The authors also gratefully acknowledge the financial and technical support from the industrial and academic members of the ThermoPlastic composites Research Center (TPRC). Further, we thank Marten van der Werff for performing the rheometry measurements on PEEK.

References

[1] A. C. Long, Composites Forming Technologies, Woodhead Publishing, Cambridge, United Kingdom, 2007.

[2] U. Sachs, Friction and Bending in Thermoplastic Composites Forming Processes, Ph.D. thesis, University of Twente, Enschede, The Netherlands, 2014.

[3] S. P. Haanappel, R. H. W. Ten Thije, U. Sachs, B. Rietman, R. Akkerman, Formability analyses of uni-directional and textile reinforced thermoplastics, Composites Part A: Applied Science and Manufacturing 56 (2014) 80–92.

[4] A. M. Murtagh, P. J. Mallon, Chapter 5 Characterisation of shearing and frictional behaviour during sheet forming, in: D. Bhattacharyya (Ed.), Composite Materials Series, volume 11, Elsevier, 1997, pp. 163–216.

[5] K. Vanclooster, Forming of Multilayered Fabric Reinforced Thermoplastic Composites, Ph.D. thesis, KU Leuven, Leuven, Belgium, 2009.

[6] R. A. Brooks, H. Wang, Z. Ding, J. Xu, Q. Song, H. Liu, J. P. Dear, N. Li, A review on stamp forming of continuous fibre-reinforced thermoplastics, International Journal of Lightweight Materials and Manufacture 5 (2022) 411–430.

[7] D. Brands, L. G. di Genova, E. R. Pierik, W. J. B. Grouve, S. Wijskamp, R. Akkerman, Formability experiments for unidirectional thermoplastics composites, in: 25th International Conference on Material Forming, Braga, Portugal: ESAFORM, 2022, pp. 1358–1371.

[8] U. Sachs, S. P. Haanappel, B. Rietman, R. H. W. Ten Thije, R. Akkerman, Formability of fiber-reinforced thermoplastics in hot press forming process based on friction properties, in: 16th International Conference on Material Forming, Aveiro, Portugal: ESAFORM, 2013, pp. 501–506.

[9] U. Sachs, R. Akkerman, Viscoelastic bending model for continuous fiber-reinforced thermoplastic composites in melt, Composites Part A: Applied Science and Manufacturing 100 (2017) 333–341.

[10] R. B. Pipes, A. Favaloro, E. Barocio, J. Hicks, Pure bending of a continuous fiber array suspended in a thermoplastic polymer in melt state, Composites Part A: Applied Science and Manufacturing 149 (2021) 106561.

[11] D. Brands, S. Wijskamp, W. J. B. Grouve, R. Akkerman, In-plane shear characterization of unidirectional fiber reinforced thermoplastic tape using the bias extension method, Frontiers in Materials 9 (2022) 863952.

[12] R. Scherer, K. Friedrich, Inter- and intraply-slip flow processes during thermoforming of CF/PP-laminates, Composites Manufacturing 2 (1991) 92–96.

[13] D. J. Groves, A. M. Bellamy, D. M. Stocks, Anisotropic rheology of continuous fibre thermoplastic composites, Composites 23 (1992) 75–80.

[14] A. M. Murtagh, M. R. Monaghan, P. J. Mallon, Investigation of the interply slip process in continous fibre thermoplastic composites, in: A. Miravete (Ed.), Proceedings of ICCM-9, Madrid, Spain: ICCM, 1993, pp. 311–318.

[15] S. R. Morris, C. T. Sun, An investigation of interply slip behaviour in AS4/PEEK at forming temperatures, Composites Manufacturing 5 (1994) 217–224.

[16] J. L. Gorczyca-Cole, J. A. Sherwood, J. Chen, A friction model for thermostamping commingled glass-polypropylene woven fabrics, Composites Part A: Applied Science and Manufacturing 38 (2007) 393–406.

[17] R. H. W. Ten Thije, R. Akkerman, M. Ubbink, L. Van der Meer, A lubrication approach to friction in thermoplastic composites forming processes, Composites Part A: Applied Science and Manufacturing 42 (2011) 950–960.

[18] K. A. Fetfatsidis, D. Jauffrès, J. A. Sherwood, J. Chen, Characterization of the tool/fabric and fabric/fabric friction for woven-fabric composites during the thermostamping process, International Journal of Material Forming 6 (2013) 209–221.

[19] U. Sachs, R. Akkerman, K. Fetfatsidis, E. Vidal-Sallé, J. Schumacher, G. Ziegmann, S. Allaoui, G. Hivet, B. Maron, K. Vanclooster, S. V. Lomov, Characterization of the dynamic friction of woven fabrics: experimental methods and benchmark results, Composites Part A: Applied Science and Manufacturing 67 (2014) 289–298.

[20] E. R. Pierik, W. J. B. Grouve, S. Wijskamp, R. Akkerman, On the origin of start-up effects in ply-ply friction for UD fiber-reinforced thermoplastics

in melt, in: 24th International Conference on Material Forming, Liège, Belgium: ESAFORM, 2021, p. 3695.

[21] E. R. Pierik, W. J. B. Grouve, S. Wijskamp, R. Akkerman, Prediction of the peak and steady-state ply-ply friction response for UD C/PAEK tapes, Composites Part A: Applied Science and Manufacturing 163 (2022) 107185.

[22] S. G. Advani, T. S. Creasy, S. F. Shuler, Chapter 8 Rheology of long fiber-reinforced composites in sheet forming, in: D. Bhattacharyya (Ed.), Composite Materials Series, volume 11, Elsevier, 1997, pp. 323–369.

[23] S. Q. Wang, Nonlinear Polymer Rheology, John Wiley & Sons, Hoboken (NJ), United States of America, 2017.

[24] B. Vergnes, Extrusion defects and flow instabilities of molten polymers, International Polymer Processing 30 (2015) 3–28.

[25] S. G. Hatzikiriakos, Wall slip of molten polymers, Progress in Polymer Science 37 (2012) 624–643.

[26] S. G. Hatzikiriakos, Appropriate boundary conditions in the flow of molten polymers, International Polymer Processing 25 (2009) 55–62.

[27] H. E. Park, S. T. Lim, F. Smillo, J. M. Dealy, Wall slip and spurt flow of polybutadiene, Journal of Rheology 52 (2008) 1201–1239.

[28] J. Xu, S. Costeux, J. M. Dealy, M. N. De Decker, Use of a sliding plate rheometer to measure the first normal stress difference at high shear rates, Rheologica Acta 46 (2007) 815–824.

[29] V. Mhetar, L. A. Archer, Slip in entangled polymer melts. 1. General features, Macromolecules 31 (1998) 8607–8616.

[30] P. E. Boukany, P. Tapadia, S. Q. Wang, Interfacial stick-slip transition in simple shear of entangled melts, Journal of Rheology 50 (2006) 641–654.

[31] A. Y. Malkin, S. A. Patlazhan, Wall slip of complex liquids - phenomenon and its causes, Advances in Colloid and Interface Science 257 (2018) 42–57.

[32] F. J. Lim, W. R. Schowalter, Wall slip of narrow molecular weight distribution polybutadienes, Journal of Rheology 33 (1989) 1359–1382.

[33] A. R. Melro, P. P. Camanho, S. T. Pinho, Generation of random distribution of fibres in long-fibre reinforced composites, Composites Science and Technology 68 (2008) 2092–2102.

[34] Toray Advanced Composites, Innovation by Chemistry, 2022. URL: `https://www.toraytac.com/`.

[35] T. Osswald, N. Rudolph, Polymer Rheology, Carl Hanser Verlag, München, Germany, 2015.

[36] F. N. Cogswell, Thermoplastic Aromatic Polymer Composites, Butterworth-Heinemann, Oxford, United Kingdom, 1992.

[37] A. Deignan, W. F. Stanley, M. A. McCarthy, Insights into wide variations in carbon fibre/polyetheretherketone rheology data under automated tape placement processing conditions, Journal of Composite Materials 52 (2017) 2213–2228.

[38] R. Akkerman, R. H. W. Ten Thije, U. Sachs, M. De Rooij, Friction in textile thermoplastic composites forming, in: Recent Advances in Textile Composites, Lille, France: TEXCOMP, 2010, pp. 271–279.

[39] R. H. W. Ten Thije, R. Akkerman, Design of an experimental setup to measure tool-ply and ply-ply friction in thermoplastic laminates, International Journal of Material Forming 2 (2009) 197–200.

[40] D. Dörr, M. Faisst, T. Joppich, C. Poppe, F. Henning, L. Kärger, Modelling approach for anisotropic inter-ply slippage in finite element forming simulation of thermoplastic UD-tapes, in: 21th International Conference on Material Forming, Palermo, Italy: ESAFORM, 2018, p. 020005.

[41] A. M. Murtagh, J. J. Lennon, P. J. Mallon, Surface friction effects related to pressforming of continuous fibre thermoplastic composites, Composites Manufacturing 6 (1995) 169–175.

[42] G. Lebrun, M. N. Bureau, J. Denault, Thermoforming-stamping of continuous glass fiber/polypropylene composites: interlaminar and tool-laminate shear properties, Journal of Thermoplastic Composite Materials 17 (2004) 137–165.

[43] Victrex plc., Shaping Future Performance, 2022. URL: `https://www.victrex.com/`.

[44] J. A. Sherwood, K. A. Fetfatsidis, J. L. Gorczyca, Chapter 6 Fabric thermostamping in polymer matrix composites, in: S. G. Advani, K. T. Hsiao (Eds.), Manufacturing techniques for polymer matrix composites (PMCs), Woodhead Publishing, 2012, pp. 139–181.

[45] P. Harrison, R. H. W. Ten Thije, R. Akkerman, A. C. Long, Characterising and modelling tool-ply friction of viscous textile composites, World Journal of Engineering 7 (2010) 5–22.

[46] S. G. Hatzikiriakos, J. M. Dealy, Wall slip of molten high density polyethylene. I. Sliding plate rheometer studies, Journal of Rheology 35 (1991) 497–523.

[47] I. B. Kazatchkov, S. G. Hatzikiriakos, Relaxation effects of slip in shear flow of linear molten polymers, Rheologica Acta 49 (2010) 267–274.

[48] P. E. Boukany, S. Q. Wang, Exploring origins of interfacial yielding and wall slip in entangled linear melts during shear or after shear cessation, Macromolecules 42 (2009) 2222–2228.

[49] L. Léger, H. Hervet, T. Charitat, V. Koutsos, The stick-slip transition in highly entangled poly(styrene-butadiene) melts, Advances in Colloid and Interface Science 94 (2001) 39–52.

[50] S. G. Hatzikiriakos, J. M. Dealy, Wall slip of molten high density polyethylenes. II. Capillary rheometer studies, Journal of Rheology 36 (1992) 703–741.

[51] S. G. Hatzikiriakos, N. Kalogerakis, Wall slip of molten high density polyethylenes. II. Capillary rheometer studies, Rheologica Acta 33 (1994) 38–47.

[52] S. G. Hatzikiriakos, J. M. Dealy, Role of slip and fracture in the oscillating flow of HDPE in a capillary, Journal of Rheology 36 (1992) 845–884.

[53] V. Mhetar, L. A. Archer, Slip in entangled polymer melts. 2. effect of surface treatment, Macromolecules 31 (1998) 8617–8622.

[54] S. Q. Wang, From wall slip to bulk shear banding in entangled polymer solutions, Macromolecular Chemistry and Physics 220 (2019).

[55] F. Brochard, P. G. de Gennes, Shear-dependent slippage at a polymer/solid surface, Langmuir 8 (1992) 3033–3037.

[56] J. Kirk, M. Kröger, P. Ilg, Surface disentanglement and slip in a polymer melt: a molecular dynamics study, Macromolecules 51 (2018) 8996–9010.

Highlights of 'Modeling the effect of temperature and pressure on the peak and steady-state ply-ply friction response for UD C/PAEK tapes':

- The ply-ply friction response can be explained with the concept of wall slip
- A higher temperature reduced the friction, without changing the slip behavior
- A higher normal pressure suppressed wall slip, increasing the steady-state friction
- The temperature- and pressure-dependency of the friction was successfully modeled

Rens Pierik: Conceptualization, Methodology, Software, Validation, Investigation, Writing – Original Draft, Visualization

Wouter Grouve: Conceptualization, Writing – Review & Editing, Supervision, Project administration, Funding acquisition.

Sebastiaan Wijskamp: Resources, Writing – Review & Editing

Remko Akkerman: Supervision, Writing – Review & Editing

Declaration of interests

☒ The authors declare that they have no known competing financial interests or personal relationships that could have appeared to influence the work reported in this paper.

☐ The authors declare the following financial interests/personal relationships which may be considered as potential competing interests: